Japanese Journal of Physiology, **36**, 43–63, 1986

Numerical Solution of Partial Differential Equations Describing the Simultaneous O_2 and CO_2 Diffusions in the Red Blood Cell

Masaji MOCHIZUKI and Tomoko KAGAWA

Department of Physiology, Yamagata University School of Medicine, Yamagata, 990–23 Japan

Abstract To describe the overall gas exchange rates in red blood cells (RBC), a computer program for solving the diffusion equations for O_2, CO_2, and HCO_3^- that accompany the chemical reactions of Bohr- and Haldane-effects was developed. Three diffusion equations were solved alternatively and repeatedly in an increment time of 2 ms. After solving the diffusion equations the P_{O_2}, O_2 saturation (S_{O_2}), P_{CO_2}, pH, and HCO_3^- content were corrected by using the Henderson-Hasselbalch equation, where the buffer value was newly derived from the CO_2 dissociation curve. In computing the Haldane effect, the buffer value was taken to be $44\,\text{mmol}\cdot l(\text{RBC})^{-1}\cdot \text{pH}_c^{-1}$, so that the change in intracellular dissolved CO_2 caused by the S_{O_2} change was fully compensated by the subsequent CO_2 diffusion. The oxygenation and deoxygenation rate factors of hemoglobin were assumed to be $2.09\cdot(1-S)^{2.02}$ and $0.3\,\text{s}^{-1}\cdot\text{Torr}^{-1}$, respectively. The P_{O_2} change due to the Bohr-shift was computed from Hill's equation, in which the K value was given by a function of the intracellular pH. When the parameter values thus far measured were used, the computed Bohr- and Haldane-effects coincided well with the experimental data, supporting the validity of the equations. The overall gas exchange profiles calculated in the pulmonary capillary model showed that the CO_2 equilibration time was significantly longer than the oxygenation time.

Key words: diffusion in red blood cell, Bohr effect, Haldane effect, overall gas exchange rate.

Under physiological conditions in the pulmonary and peripheral capillaries, the O_2 and CO_2 diffusions into and out of the red blood cells (RBC) are mutually influenced by the Bohr- and Haldane-effects. To estimate the overall gas exchange rate, the oxygenation and deoxygenation rates as well as the CO_2 and HCO_3^- diffusion rates in the RBC must be solved simultaneously. However, because of

Received for publication October 16, 1985

difficulty in solving the diffusion equations in the RBC model, the above rates have theoretically not yet been clarified. In the previous papers (KAGAWA and MOCHIZUKI, 1982, 1984), we developed programs to compute the oxygenation rate and CO_2 and HCO_3^- diffusion rates in the RBC. In this study, we developed equations for simultaneous O_2 and CO_2 diffusion including the HCO_3^- shift, and Bohr- and Haldane-effects. Furthermore, the validity of the diffusion equations of O_2, CO_2, and HCO_3^- and the assumptions made in computing the Bohr- and Haldane-effects were tested by comparing the calculated profiles of intra- and extracellular P_{O_2} and P_{CO_2} with the experimental data.

DETERMINATION OF PARAMETER VALUES

The diffusion coefficients of O_2, CO_2, and HCO_3^- within the RBC and the permeabilities across the barrier around RBC were cited from previous experimental data (KAGAWA and MOCHIZUKI, 1982; UCHIDA *et al.*, 1983; NIIZEKI *et al.*, 1983, 1984). The oxygenation rate factor of hemoglobin, $F_s(\mathrm{ox})$, was taken to be $2.09\cdot(1-S)^{2.02}\,\mathrm{s}^{-1}\cdot\mathrm{Torr}^{-1}$ according to MOCHIZUKI (1966a), MOCHIZUKI *et al.* (1966) and KAGAWA and MOCHIZUKI (1982), where S is the O_2-saturation value. As new parameter values, the deoxygenation rate factor of hemoglobin, the buffer value and Donnan ratio were introduced.

1) Deoxygenation rate constant. The O_2 diffusion accompanying the deoxygenation reaction in a disc RBC model is given by an equation similar to that of the oxygenation reaction (MOCHIZUKI and FUKUOKA, 1958; MOCHIZUKI, 1975) and stated as follows:

$$\alpha(O_2)\frac{\partial P_{O_2}}{\partial t}=\alpha(O_2)D(O_2)\left(\frac{\partial^2 P_{O_2}}{\partial r^2}+\frac{1}{r}\frac{\partial P_{O_2}}{\partial r}+\frac{\partial^2 P_{O_2}}{\partial z^2}\right)+F_s(\mathrm{deox})(P_{O_2}{}^*-P_{O_2}), \qquad (1)$$

where $\alpha(O_2)$ and $D(O_2)$ are the solubility and diffusion coefficient of O_2 in the RBC, $F_s(\mathrm{deox})$ is the deoxygenation rate factor of hemoglobin and $P_{O_2}{}^*$, calculated from Hills' equation, is the P_{O_2} equilibrated with a given O_2-saturation value. Using the same boundary conditions and parameter values as described in the foregoing paper (KAGAWA and MOCHIZUKI, 1982), Eq. (1) is solved and $F_s(\mathrm{deox})$ is determined by comparing the computed S_{O_2}-time curves with the experimental data. MOCHIZUKI (1966b) measured the deoxygenation rate by using a rapid flow method in RBC suspension with a fractional hematocrit of 0.13×10^{-2}. Assuming that the transfer coefficient of O_2 across the boundary layer around the RBC, $\eta(O_2)$, is independent of the direction of diffusion, the $\eta(O_2)$ was taken to be $2.5\times10^{-6}\,\mathrm{cm}\cdot\mathrm{s}^{-1}\cdot\mathrm{Torr}^{-1}$, similar to that used in oxygenation. The other parameter values used are tabulated in Table 1.

The computed and experimental S_{O_2}-time curves were in strong agreement, when $F_s(\mathrm{deox})=0.3\,\mathrm{s}^{-1}\cdot\mathrm{Torr}^{-1}$ was used. Figure 1 shows three S_{O_2}-time curves computed at three different experimental conditions, where the radius, c, and thickness, d, of the RBC were assumed to be 3.5 and 1.6 μm, respectively. The

Table 1. Notations used in the equations.

Notations	Parameters and their dimensions
$C_b(CO_2)$	CO_2 content in blood (mmol·l (blood)$^{-1}$)
c	radius of the RBC model ($=3.5\times10^{-4}$ cm)
$2d$	thickness of the RBC model ($=1.6\times10^{-4}$ cm)
$D(O_2)$	diffusion coefficient of O_2 in RBC ($=0.46\times10^{-5}$ cm^2·s^{-1})
$D(CO_2)$	diffusion coefficient of CO_2 in RBC ($=0.34\times10^{-5}$ cm^2·s^{-1})
$D(HCO_3^-)$	diffusion coefficient of HCO_3^- in RBC ($=0.14\times10^{-5}$ cm^2·s^{-1})
F_s(deox)	deoxygenation rate of hemoglobin ($=0.3$ s^{-1}·Torr^{-1})
F_s(ox)	oxygenation rate of hemoglobin ($=2.09\ (1-S)^{2.02}$ s^{-1}·Torr^{-1})
$(HCO_3^-)_c$	intracellular HCO_3^- content (mmol·l (RBC)$^{-1}$)
$(HCO_3^-)_p$	extracellular HCO_3^- content (mmol·l (plasma)$^{-1}$)
HE	CO_2 content in the Haldane effect (mmol·l (RBC)$^{-1}$)
Ht	fractional hematocrit
K	K-value in Hill's equation of O_2 dissociation curve
N	O_2 capacity of RBC ($=0.43$)
n	n-value in Hill's equation of O_2 dissociation curve
P_{O_2}	intracellular P_{O_2} (Torr)
P_{O_2}*	O_2-back-pressure (Torr)
P_{O_2}(P)	extracellular P_{O_2} (Torr)
P_{50}	P_{O_2} at $S_{O_2}=0.5$ (Torr)
P_{CO_2}	intracellular P_{CO_2} (Torr)
P_{CO_2}(P)	extracellular P_{CO_2} (Torr)
pH_c	intracellular pH
pH_p	extracellular pH
pH_b*	extracellular pH corresponding to the amount of buffer base of plasma protein BP_s
R	carbamate fraction in the Haldane effect (Eq. 4)
r	radial distance in RBC
S	fractional O_2 saturation
TC	time constant of carbonic anhydrase activity in plasma
t	time
z	vertical distance in RBC
$\alpha(O_2)$	O_2 solubility in RBC ($=0.31\times10^{-4}$ Torr^{-1})
$\alpha_c(CO_2)$	CO_2 solubility in RBC ($=0.0262$ mmol·l (RBC)$^{-1}$·Torr^{-1})
$\alpha_p(CO_2)$	CO_2 solubility in plasma ($=0.0308$ mmol·l (plasma)$^{-1}$·Torr^{-1})
β_c	buffer value of hemoglobin (Eq. 8)
β_c*	buffer value of hemoglobin by Haldane effect ($=44$ mmol·l (RBC)$^{-1}$·pH_c^{-1})
β_p	buffer value of plasma protein ($=7.0$ mmol·l (plasma)$^{-1}$·pH^{-1})
$\eta(O_2)$	transfer coefficient of O_2 ($=2.5\times10^{-6}$ cm·s^{-1}·Torr^{-1})
$\eta(CO_2)$	transfer coefficient of CO_2 ($=2.5\times10^{-6}$ cm·s^{-1}·Torr^{-1})
$\eta(HCO_3^-)$	transfer coefficient of HCO_3^- (outward: 7×10^{-4} cm·s^{-1}, inward: 5×10^{-4} cm·s^{-1})
γ	Donnan ratio (Eq. 9)
λ'	ratio of extracellular HCO_3^- to the total, (HE$-R$), in the Haldane effect
$(1-\lambda')$	ratio of intracellular HCO_3^- to (HE$-R$) in the Haldane effect

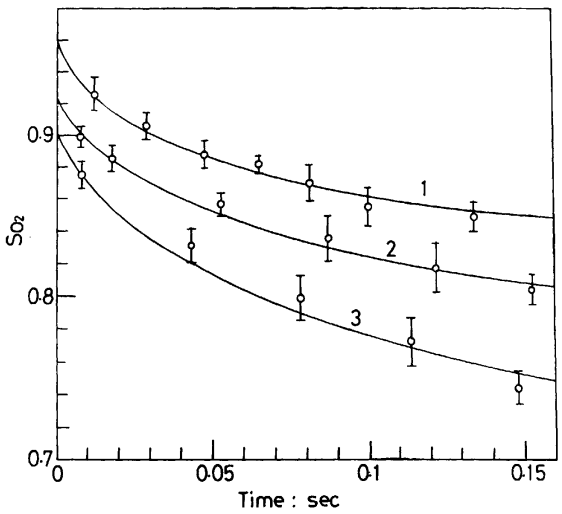

Fig. 1. S_{O_2}-time curves during the deoxygenation. The solid lines were computed in a closed RBC suspension at a hematocrit value of 0.13×10^{-2}. The initial conditions are the same as those in the experiment, where $F_s(\text{deox}) = 0.3\,s^{-1} \cdot \text{Torr}^{-1}$ and $\eta(O_2) = 2.5 \times 10^{-6}\,\text{cm}^{-1} \cdot s^{-1} \cdot \text{Torr}^{-1}$. The plotted points and bars are the mean and S.D. of S_{O_2} measured at 37°C during the deoxygenation (MOCHIZUKI, 1966b).

intracellular P_{O_2} in the first to third experiments was 88, 68, and 61 Torr, and the extracellular P_{O_2} was 45, 38, and 30 Torr, respectively. These curves indicate the accuracy of the F_s(deox) value.

2) Buffer value of hemoglobin and related parameters. From the relationship between the P_{CO_2} and HCO_3^- content in whole blood and true plasma measured in human subjects by TAZAWA *et al.* (1983), we derived the formulas for intra- and extracellular HCO_3^- concentrations of oxygenated blood, $(HCO_3^-)_c(ox)$ and $(HCO_3^-)_p(ox)$, as follows:

$$(HCO_3^-)_c(ox) = 11.9 + 0.16 \cdot (P_{CO_2} - 40) - 0.14 \times 10^{-2} \cdot (P_{CO_2} - 40)^2 \quad (\text{mmol} \cdot l(\text{RBC})^{-1}), \tag{2}$$

and

$$(HCO_3^-)_p(ox) = 6.72 \cdot P_{CO_2}^{0.34} \quad (\text{mmol} \cdot l(\text{plasma})^{-1}). \tag{3}$$

The carbamate and intra- and extracellular HCO_3^- components in the Haldane effect were then obtained from the CO_2 dissociation curves of oxygenated and deoxygenated blood and true plasma. The estimation was done by using the Henderson-Hasselbalch equation, as described by MOCHIZUKI *et al.* (1983b). The carbamate CO_2-content in Haldane effect, R, was given by

$$R=2.451+0.757\times10^{-2}\cdot(P_{CO_2}-40)$$
$$-1.15\times10^{-4}\cdot(P_{CO_2}-40)^2 \qquad (\text{mmol}\cdot l(\text{RBC})^{-1}) . \tag{4}$$

The carbamate CO_2-content in the oxygenated blood was assumed to be $0.9\,\text{mmol}\cdot l(\text{RBC})^{-1}$ regardless of the P_{CO_2} value by referring to the data of BAUER and SCHRÖDER (1972). The intra- and extracellular HCO_3^- fractions of the Haldane effect were given by

$$(1-\lambda')(\text{HE}-R)=0.903+0.012\cdot(P_{CO_2}-40)$$
$$-0.18\times10^{-3}\cdot(P_{CO_2}-40)^2 \qquad (\text{mmol}\cdot l(\text{RBC})^{-1}) , \tag{5}$$

and

$$\lambda'\cdot(\text{HE}-R)=2.33-0.33\times10^{-2}\cdot(P_{CO_2}-40)$$
$$-0.3\times10^{-4}\cdot(P_{CO_2}-40)^2 \qquad (\text{mmol}\cdot l(\text{RBC})^{-1}) . \tag{6}$$

where HE and λ' are the CO_2 content change caused by a complete change in S_{O_2} (Haldane effect) and the partition coefficient of HCO_3^- ions between RBC and plasma in the Haldane effect.

The intracellular pH, pH_c, was calculated from the $(HCO_3^-)_c$ and P_{CO_2} by using $pK'=6.1$, according to BAUER and SCHRÖDER (1972) and stated as:

$$pH_c=6.1+\log\{(HCO_3^-)_c/(0.0262\times P_{CO_2})\} . \tag{7}$$

From Eqs. (2) to (7), the buffer value of oxygenated hemoglobin, β_c, was derived by dividing the change in HCO_3^- content by that in intracellular pH, as:

$$\beta_c=62.03-41.43\cdot(pH_c-7.17)$$
$$-92.04\cdot(pH_c-7.17)^2 \qquad (\text{mmol}\cdot l(\text{RBC})^{-1}\cdot pH_c^{-1}) . \tag{8}$$

Furthermore, the Donnan ratio, γ, for HCO_3^- was evaluated as

$$\gamma=0.5-0.47\cdot(pH_c-7.17)-0.76\cdot(pH_c-7.17)^2$$
$$(l(\text{plasma})\cdot l(\text{RBC})^{-1}) . \tag{9}$$

In their data, the Donnan ratio was independent of the S_{O_2} value.

3) O_2 dissociation curve. The Bohr-effect coefficient in human blood has usually been expressed by (BAUER, 1974)

$$\Delta\log P_{50}/\Delta pH_p=-0.48 , \tag{10}$$

where P_{50} is the P_{O_2} at $S=0.5$ on the O_2-dissociation curve. The P_{50} at $pH_p=7.4$ is approximately 26.5 Torr. The relationship between the pH_p and pH_c is given from Eqs. (2), (3), and (7) by

$$pH_c=7.17+0.72\cdot(pH_p-7.4)-0.27\cdot(pH_p-7.4)^2 . \tag{11}$$

Since the O_2 dissociation curve is approximated by Hills' equation as

$$S = K \cdot P_{O_2}{}^n / (1 + K \cdot P_{O_2}{}^n) . \quad (12)$$

The relation between the K-value of Eq. (12) and the pH_c can be estimated from Eqs. (10) and (11). Assuming the n-value to be 2.5, $\log K$ is linearly related to the pH_c as follows:

$$\log K = 1.68 \cdot (pH_c - 7.17) - 3.555 . \quad (13)$$

The O_2 dissociation curve computed from Eq. (12) by using the K of Eq. (13) strongly agreed with the standard O_2 dissociation curve reported by BARTELS *et al.* (1961).

FORMULAS FOR CORRECTING INTRA- AND EXTRACELLULAR P_{CO_2} AND HCO_3^- CONTENT

Before programming the formulas for correcting the intracellular P_{CO_2}, the HCO_3^- changes due to CO_2 hydration or dehydration reaction and the Haldane effect were determined. Then, the formulas for computing the change in extracellular HCO_3^- content due to the buffer action of plasma protein were derived, taking the carbonic anhydrase activity in the capillary wall into consideration.

1) Intracellular P_{CO_2} change due to the HCO_3^- shift and Haldane effect. In the RBC, the CO_2 hydration or dehydration reaction occurs with the change in P_{CO_2} and HCO_3^- values, as shown by NIIZEKI *et al.* (1983, 1984). Assuming that the carbonic anhydrase activity in the RBC is so high that the above reaction is completed in 1 ms, the changes in intracellular P_{CO_2} and HCO_3^- are calculated by using the following equation (SHIMOUCHI *et al.*, 1984; KAGAWA and MOCHIZUKI, 1984):

$$\log\left(1 + \frac{\Delta P_{CO_2}{}^* - \Delta P_{CO_2}}{P_{CO_2}(i)}\right) = \frac{\alpha_c(CO_2) \cdot \Delta P_{CO_2}}{\beta_c} + \log\left(1 + \frac{\alpha_c(CO_2) \cdot \Delta P_{CO_2}}{(HCO_3^-)_c(i)}\right), \quad (14a)$$

or

$$\log\left(1 + \frac{\Delta(HCO_3^-)_c}{\alpha_c(CO_2) \cdot \Delta P_{CO_2}(i)}\right) = -\frac{\Delta(HCO_3^-)_c}{\beta_c} + \log\left(1 + \frac{\Delta(HCO_3^-)_c{}^* - \Delta(HCO_3^-)_c}{(HCO_3^-)_c(i)}\right). \quad (14b)$$

$\Delta P_{CO_2}{}^*$ and $\Delta(HCO_3^-)_c{}^*$ in the above equation are the primary P_{CO_2} and HCO_3^- changes caused by CO_2 diffusion and the HCO_3^- shift. $\Delta P_{CO_2}{}^*$ and ΔP_{CO_2}, and also $\Delta(HCO_3^-)_c{}^*$ and $\Delta(HCO_3^-)_c$ should have the same + or − sign. $\alpha_c(CO_2)$ represents intracellular CO_2 solubility. $P_{CO_2}(i)$ and $(HCO_3^-)_c(i)$ are those values at the i'th increment time.

The intracellular P_{CO_2} and HCO_3^- changes that take place are also due to the change in S_{O_2}, i.e., the Haldane effect. When the deoxygenation reaction proceeds in the closed RBC, the HCO_3^- and carbamate concentrations increase, decreasing the P_{CO_2} thereof. If no dehydration reaction in HCO_3^- ion occurs during the

deoxygenation process, the intracellular P_{CO_2} may drop by the amount of $\Delta P_{CO_2}{}^*$ as given by

$$\Delta P_{CO_2}{}^* = HE \cdot \Delta S / \alpha_c(CO_2) . \tag{15}$$

However, following the decrease in P_{CO_2}, HCO_3^- dehydration occurs, reducing $(HCO_3^-)_c$ and moderating the P_{CO_2} drop. Let the dehydrated HCO_3^- quantity be $\Delta(HCO_3^-)_c$, as described in Eq. (14b). Then, the decrease of P_{CO_2} in Eq. (15) is corrected by $\Delta(HCO_3^-)_c/\alpha_c(CO_2)$, resulting in the following P_{CO_2} drop:

$$\Delta P_{CO_2} = \{HE \cdot \Delta S - \Delta(HCO_3^-)_c\}/\alpha_c(CO_2) . \tag{16}$$

The intracellular HCO_3^- change due to the Haldane effect, $(HE - R) \cdot \Delta S$ is also moderated by the dehydration reaction as much as $\Delta(HCO_3^-)_c$, yielding the net change, $(HE - R) \cdot \Delta S - \Delta(HCO_3^-)_c$. In the above example of the deoxygenation process, the change in S_{O_2}, ΔS is negative, and therefore, $\Delta(HCO_3^-)_c$ is also negative. In contrast, during the oxygenation process, both the ΔS and $\Delta(HCO_3^-)_c$ are positive. On the other hand, let the buffer value for the Haldane effect be $\beta_c{}^*$. Then, the change in pH_c caused by the Haldane effect may be given according to VAN SLYKE *et al.* (1923) by

$$-\Delta pH_c = \Delta(HCO_3^-)_c/\beta_c{}^* . \tag{17}$$

Thus, similar to Eq. (14), the relation between pH_c, P_{CO_2}, and HCO_3^- content in the RBC expressed from Eqs. (16) and (17) as

$$\log\left(1 + \frac{HE \cdot \Delta S - \Delta(HCO_3^-)_c}{\alpha_c(CO_2) \cdot P_{CO_2}(i)}\right) = \frac{\Delta(HCO_3^-)_c}{\beta_c{}^*} + \log\left(1 - \frac{(HE - R) \cdot \Delta S - \Delta(HCO_3^-)_c}{(HCO_3^-)_c(i)}\right). \tag{18}$$

When the β_c of Eq. (8) was used in Eq. (18) instead of $\beta_c{}^*$, the CO_2 diffusion quantity computed by varying the S_{O_2} with the same extracellular P_{CO_2} became about 40% smaller than the total change in carbamate and HCO_3^- given by the initial conditions, i.e., $HE \cdot \Delta S$. When $\beta_c{}^* = 44\,\text{mmol} \cdot l(RBC)^{-1} \cdot pH_c{}^{-1}$, strong agreement was observed between $HE \cdot \Delta S$ and the subsequent CO_2 diffusion quantity. Thus, in the following computation, the above $\beta_c{}^*$ value was invariably used together with Eq. (18).

2) Extracellular P_{CO_2} and HCO_3^- changes due to buffering of plasma protein. The buffering rate of plasma protein is limited by the carbonic anhydrase activity in the capillary wall. According to KLOCKE (1978) the time constant of the buffering rate is in the range of 1 to 2 s. Let the buffer base value of plasma protein at the final equilibrium state and at any time during the reaction be $BP_s(\infty)$ and $BP_s(t)$. Then, the change in BP_s may be approximated by using the time constant, TC, as

$$dBP_s/dt = \{BP_s(\infty) - BP_s(t)\}/TC . \tag{19}$$

According to VAN SLYKE *et al.* (1923, 1928), the amount of BP_s is linearly related to the extracellular pH. Let the buffer value of plasma protein be β_p, which has been approximated to be $7\,\text{mmol}\cdot l(\text{plasma})^{-1}\cdot pH_p^{-1}$. Then, Eq. (19) is rewritten by the following equation:

$$\beta_p \frac{dpH_p^*}{dt} = \beta_p\{pH_p(\infty) - pH_p^*(i)\}/TC\,, \tag{20}$$

where $pH_p^*(i)$ is the pH_p on the BP_s-pH_p line corresponding to the BP_s value at the i'th increment time. Because the pH_p^* should approach the actual pH_p at the final equilibrium state or $t=\infty$, $pH_p(\infty)$ is taken to be equal to the actual $pH_p(i)$ at the i'th increment time, which is calculated from the Henderson-Hasselbalch equation by using P_{CO_2} and $(HCO_3^-)_p$. In other words, Eq. (20) is rewritten as:

$$\frac{\Delta(HCO_3^-)_p^*(i)}{\Delta t} = \frac{\beta_p}{TC}\{pH_p(i) - pH_p^*(i)\}\,, \tag{21}$$

where $\Delta(HCO_3^-)_p^*$ is the change in extracellular HCO_3^- caused by the buffer action of plasma protein. Starting from $pH_p(0)$, the $pH_p^*(i)$ is calculated successively as given by the equation:

$$pH_p^*(i) = pH_p^*(i-1) + \Delta(HCO_3^-)_p^*(i)/\beta_p\,. \tag{22}$$

On the other hand, the extracellular HCO_3^- concentration using the new increment time was calculated by adding $\Delta(HCO_3^-)_p^*$(i) together with the HCO_3^- diffusion quantity out of the RBC to the HCO_3^- concentration at the old time.

PROGRAMMING OF DIFFUSION EQUATIONS

The program for the numerical solution consisted of 12 major steps. The flow chart is shown in Fig. 2. The increment time was 2 ms, during which all the equations were computed sequentially. First, (*1*), the CO_2 diffusion equation was solved by using the same program as shown in the preceding paper, that is, the alternating-direction-implicit method (DOUGLAS and RACHFORD, 1956). Then, (*2*), the changes in P_{CO_2} and HCO_3^- due to hydration or dehydration were computed by using the modified Henderson-Hasselbalch equation, Eq. (14), to correct the changes in P_{CO_2} and HCO_3^-. From the new P_{CO_2} and HCO_3^- values, (*3*), the intracellular pH was computed from Eq. (7). Then, the γ-value was computed from Eq. (9), and further (*4*), $\log K$ was calculated from Eq. (13). By inserting the corrected K-value to Eq. (12), (*5*), the $P_{O_2}^*$ which will be referred to as the O_2-back-pressure, is calculated. Assuming that the change in $P_{O_2}^*$ due to the Bohr effect is the same as that of the actual intracellular P_{O_2}, the intracellular P_{O_2} due to the Bohr shift was computed as

$$P_{O_2}(i) = P_{O_2}(i-1) + \Delta P_{O_2}^*(i)\,. \tag{23}$$

By inserting the new P_{O_2} of Eq. (23) into the program of the O_2 diffusion, (*6*),

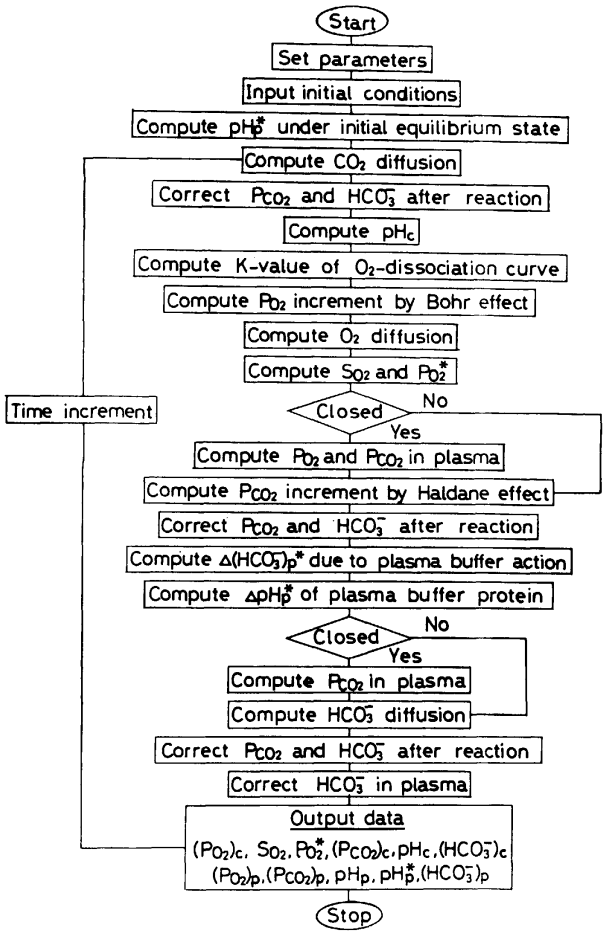

Fig. 2. Flow-chart of the computer program for simultaneous O_2, CO_2, and HCO_3^- diffusions in the RBC. Extracellular CO_2 hydration or dehydration reaction is included.

the O_2 diffusion equation was solved. Subsequently, (*7*), the change in S_{O2}, ΔS was computed by using the following equation:

$$\Delta S = F_s(\text{ox or deox})\{P_{O_2}(i) - P_{O_2}{}^*(i)\}\Delta t/N\,. \tag{24}$$

where N is the O_2 capacity of the RBC. Inserting ΔS into Eq. (18), the intracellular P_{CO_2} and HCO_3^- changes due to the Haldane effect were computed. Then, (*8*), the change in extracellular HCO_3^- due to the buffer action of the plasma protein was calculated from Eq. (21) where the time constant, TC, was usually taken to be 1.5 s. The $(HCO_3^-)_p$ was corrected by adding the above HCO_3^- change, $\Delta(HCO_3^-)_p{}^*$ to it. Furthermore, from Eq. (22) the $pH_p{}^*(i)$ was calculated. After correcting the extracellular HCO_3^-, pH_p, and $pH_p{}^*$ values, (*9*), the diffusion equation for HCO_3^- was solved. By using the modified Henderson-Hasselbalch equation, Eq. (14), (*10*),

the P_{O_2} and HCO_3^- changes caused by the HCO_3^- shift were corrected. Then, (*11*), the total CO_2 in blood was calculated by

$$C_b(CO_2) = Ht \cdot \{(HCO_3^-)_c + 0.9 + R \cdot (1 - S)\} + (1 - Ht) \cdot (HCO_3^-)_p + \{Ht \cdot \alpha_c(CO_2) + (1 - Ht) \cdot \alpha_p(CO_2)\} \cdot P_{CO_2} \quad (mmol \cdot l(blood)^{-1}). \quad (25)$$

After these computations, (*12*), the P_{CO_2}, HCO_3^-, CO_2 content, pH, P_{O_2}*, and S_{O_2} were printed out every 10 ms.

In the open system, the extracellular P_{CO_2} and P_{O_2} were kept constant, whereas the HCO_3^- content was altered. In the closed system, the extracellular P_{CO_2}, P_{O_2}, and HCO_3^- content were corrected after the CO_2, O_2, and HCO_3^- diffusions. The equations used for the correction have been described previously (KAGAWA and MOCHIZUKI, 1984).

The O_2 and CO_2 solubilities, the diffusion and transfer coefficients of O_2, CO_2, and HCO_3^-, and all other parameters are tabulated in Table 1. They are similar to those used in the previous studies (KAGAWA and MOCHIZUKI, 1982, 1984). In Kagawa's paper on computer programs (KAGAWA, 1984), the parameters relating to the CO_2 dissociation curve were not all compatible with previous experimental data (MOCHIZUKI *et al.*, 1983b). Thus, we used a quadratic equation such as Eq. (2) for intracellular HCO_3^- and expressed the β_c value as a dependent variable of the pH_c, as in Eq. (8). The equations used for the initial intra- and extracellular HCO_3^- contents are tabulated in Table 2 together with the equations described above.

Table 2. Formulas for calculating parameter values.

Parameters	Eq. No.	Formulas
$(HCO_3^-)_c$		$(HCO_3^-)_c = (HCO_3^-)_c(ox) + (1 - S)(1 - \lambda')(HE - R)$
$(HCO_3^-)_c(ox)$	2	$(HCO_3^-)_c(ox) = 11.9 + 0.16 \cdot (P_{CO_2} - 40) - 0.14 \times 10^{-2} \cdot (P_{CO_2} - 40)^2$
RBC HCO_3^- in Haldane effect	5	$(1 - \lambda')(HE - R) = 0.903 + 0.012 \cdot (P_{CO_2} - 40) - 0.18 \times 10^{-3} \cdot (P_{CO_2} - 40)^2$
$(HCO_3^-)_p$		$(HCO_3^-)_p = (HCO_3^-)_p(ox) + (1 - S)\lambda'(HE - R)Ht/(1 - Ht)$
$(HCO_3^-)_p(ox)$	3	$(HCO_3^-)_p(ox) = 6.72 \cdot P_{CO_2}^{0.34}$
Plasma HCO_3^- in Haldane effect	6	$\lambda'(HE - R) = 2.33 - 0.33 \times 10^{-2} \cdot (P_{CO_2} - 40) - 0.3 \times 10^{-4} \cdot (P_{CO_2} - 40)^2$
Carbamate, R	4	$R = 2.451 + 0.757 \times 10^{-2} \cdot (P_{CO_2} - 40) - 1.15 \times 10^{-4} \cdot (P_{CO_2} - 40)^2$
Blood C_{CO_2}	25	$C_b(CO_2) = Ht \cdot \{(HCO_3^-)_c + 0.9 + R \cdot (1 - S)\} + (1 - Ht) \cdot (HCO_3^-)_p + \{Ht \cdot \alpha_c(CO_2) + (1 - Ht) \cdot \alpha_p(CO_2)\} \cdot P_{CO_2}$
Donnan ratio, γ	9	$\gamma = 0.5 - 0.47 \cdot (pH_c - 7.17) - 0.76 \cdot (pH_c - 7.17)^2$
Buffer value, β_c	8	$\beta_c = 62.03 - 41.43 \cdot (pH_c - 7.17) - 92.04 \cdot (pH_c - 7.17)^2$
K of Hill's equation	13	$\log K = 1.68 \cdot (pH_c - 7.17) - 3.555$

RESULTS

1) Changes in P_{CO_2} and CO_2 content due to the Haldane effect

To confirm the validity of Eq. (18) for the Haldane effect, we calculated the change in CO_2 content during the oxygenation at four P_{CO_2} levels ranging from 30 to 60 Torr. The initial conditions and predicted final S_{O_2} value and CO_2 content, C_{CO_2}, are tabulated in Table 3. The S_{O_2} value varied from 0.43 to 0.95. The calculated CO_2 content is illustrated in Fig. 3. The solid curves are the CO_2 values computed by inserting $\beta_c^* = 44\,\text{mmol}\cdot l(\text{RBC})^{-1}\cdot \text{pH}_c^{-1}$ into Eq. (18). The broken lines are the CO_2 contents at the final equailibrium state. Strong agreement was observed between the solid and broken lines, with a reaction time of 1 s. The half-times ranged from 0.24 to 0.18 s, being reduced as the P_{CO_2} increased.

KLOCKE (1973) measured the extracellular P_{CO_2} change due to the Haldane effect by means of a rapid flow method. To compare our computed data with his measured values, we calculated the overall gas exchange profile in a closed system for his experimental conditions. The hematocrit of the RBC suspension was 0.025, and the initial intra- and extracellular P_{O_2} were 10 and 165 Torr, respectively, whereas both the intra- and extracellular P_{CO_2} values were equally 40 Torr at the initial stage. Figure 4 shows the changes in intra- and extracellular P_{CO_2} together with the experimental data. Immediately after mixing, the S_{O_2} rose from 0.084 to 0.830 and the intracellular P_{CO_2} also showed a high initial peak, as shown by the broken curve in the figure. Following the change in intracellular P_{CO_2}, the extracellular P_{CO_2} increased, as the outward CO_2 diffusion proceeded and the intracellular P_{CO_2} decreased. The half-time of the extracellular P_{CO_2} curve was about 0.15 s, and coincided well with the experimental value, as shown in Fig. 4.

Table 3. Initial and boundary conditions for computing the rate of the Haldane effect and the half-time of the CO_2 change.

Parameters	Dimension	P_{CO_2} (Torr)			
		30	40	50	60
Initial $(P_{O_2})_c$	Torr	21.48	23.47	25.27	26.93
Initial $(P_{O_2})_p$	Torr	82.22	89.88	96.73	103.02
Initial S_{O_2}	%	43.05	43.05	43.05	43.05
Final S_{O_2}	%	95.22	95.25	95.27	95.29
Initial $(HCO_3^-)_c$	$\text{mmol}\cdot l\,(\text{RBC})^{-1}$	10.63	12.42	13.91	15.18
Initial $(HCO_3^-)_p$	$\text{mmol}\cdot l\,(\text{plasma})^{-1}$	22.46	24.64	26.48	28.09
Initial C_{CO_2}	$\text{mmol}\cdot l\,(\text{blood})^{-1}$	19.01	21.32	23.31	25.06
Final C_{CO_2}	$\text{mmol}\cdot l\,(\text{blood})^{-1}$	17.70	19.96	21.92	23.66
C_{CO_2} at 1 s	$\text{mmol}\cdot l\,(\text{blood})^{-1}$	17.76	20.00	21.97	23.72
$t_{1/2}$	s	0.240	0.213	0.192	0.175

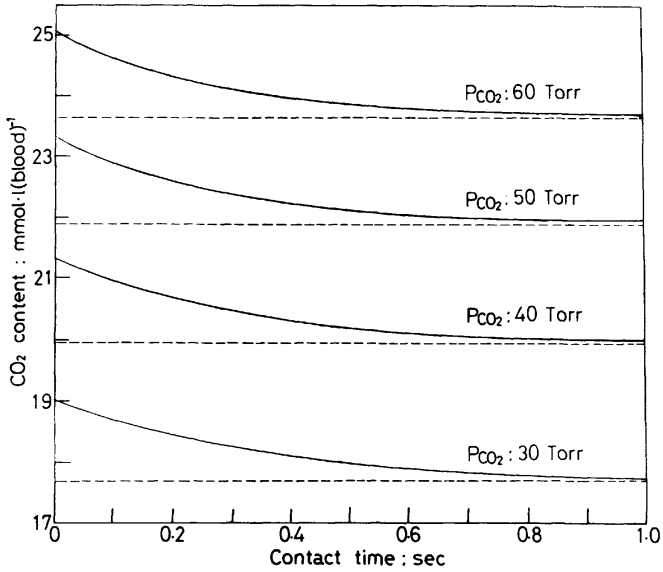

Fig. 3. Change in CO_2 content due to the Haldane effect computed at 4 different P_{CO_2} levels between 30 and 60 Torr. The S_{O_2} was changed from 0.43 to 0.95 by an increase in extracellular P_{O_2}. The solid curve was computed by using Eq. (18). The broken line represents the final CO_2 content predicted from the CO_2 dissociation curve.

2) Changes in P_{O_2} and S_{O_2} due to the Bohr effect

The validity of the assumption of Eq. (23), which defines the P_{O_2} changes due to the Bohr shift, was then checked by computing the decrease in S_{O_2} in an open system and also the increase in extracellular P_{O_2} in a closed system. The profiles of P_{CO_2}, HCO_3^- content, P_{O_2}* and S_{O_2}, and pH obtained in the open system by increasing the extracellular P_{CO_2} from 30 to 50 Torr are illustrated in the graphs of A, B, C, and D of Fig. 5, respectively. Because the pH_c decreased with an increase in P_{CO_2}, the intracellular P_{O_2} as well as the O_2 back-pressure, P_{O_2}*, increased, causing outward O_2 diffusion or deoxygenation. As shown by the chain line in Fig. 5C, S_{O_2} decreased from 0.63 to 0.54 during the 1 s reaction time. The Bohr-off-shift generally depends on the extracellular P_{O_2}, or the S_{O_2} range. In the case of Fig. 5, the half-time of the S_{O_2} change was about 390 ms. As the pH_c decreases from 7.225 to 7.117, P_{O_2}* first increased by 2.3 Torr, and then, after showing a peak, gradually decreased. The half-time of the intracellular HCO_3^- was about 50 ms, whereas that of the extracellular HCO_3^- was about 170 ms. Because the extracellular P_{CO_2} was raised at the initial stage of from 30 to 50 Torr, the pH_p decreased from 7.478 to 7.256, but then, increased as shown by the solid curve in Fig. 5D.

In order to compare the rate of the above Bohr-off-shift with that of the deoxygenation reaction, we computed the S_{O_2} due to deoxygenation over a similar S_{O_2} range by reducing the extracellular P_{O_2} from 26 to 21.7 Torr. The extracellular

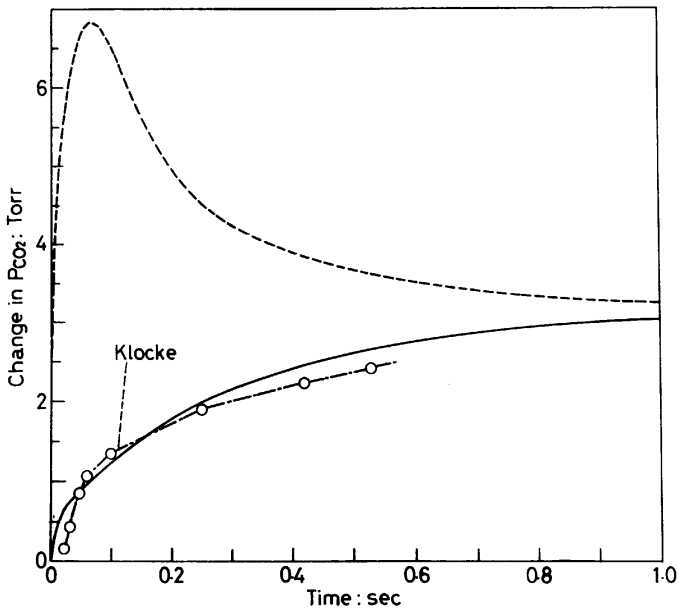

Fig. 4. Changes in intra- and extracellular P_{CO_2} computed in the Haldane effect. The initial P_{O_2} in RBC and extracellular fluid are 10 and 165 Torr, and the initial P_{CO_2} is 41 Torr. The hematocrit is 0.025. The plotted points are replotted from the experimental data of KLOCKE (1973).

P_{CO_2} was kept constant at 35 Torr. The S_{O_2} change shown in Fig. 6C by the chain line had a half-time of about 290 ms, which is about 3/4 that of the Bohr-off-shift in Fig. 5. According to the Haldane effect, the intracallular P_{CO_2} decreases by 0.36 Torr at the peak, causing the inward CO_2 diffusion and an increase in HCO_3^- concentration. MOCHIZUKI *et al.* (1983a) measured the Bohr-off-shift together with the deoxygenation reaction in an open system by using a microphotometric method. The shortest half-times of the Bohr-off-shift and the deoxygenation in their measurements were about 400 and 300 ms, respectively, indicating the validity of our equations.

The Bohr-off-shift was measured by CRAW *et al.* (1963), NAKAMURA and STAUB (1964), and FORSTER and STEEN (1968): They observed the change in extracellular P_{O_2} in a closed reaction chamber after changing the extracellular P_{CO_2}. The half-time of the intracellular P_{O_2} change is in general shorter in a closed system than in an open system. In addition, the half-time of the S_{O_2} change at a high S_{O_2} range is shorter than at a low S_{O_2} range because of the non-linear characteristic of the O_2 dissociation curve. In order to clarify the S_{O_2} dependency in terms of half-time, we calculated the Bohr-off-shift at various P_{O_2} levels of 30 to 90 Torr by changing the intracellular P_{CO_2} from 40 to 60 Torr at a constant hematocrit of 0.015, referring to NAKAMURA and STAUB (1964) and FORSTER and STEEN (1968). The initial in-

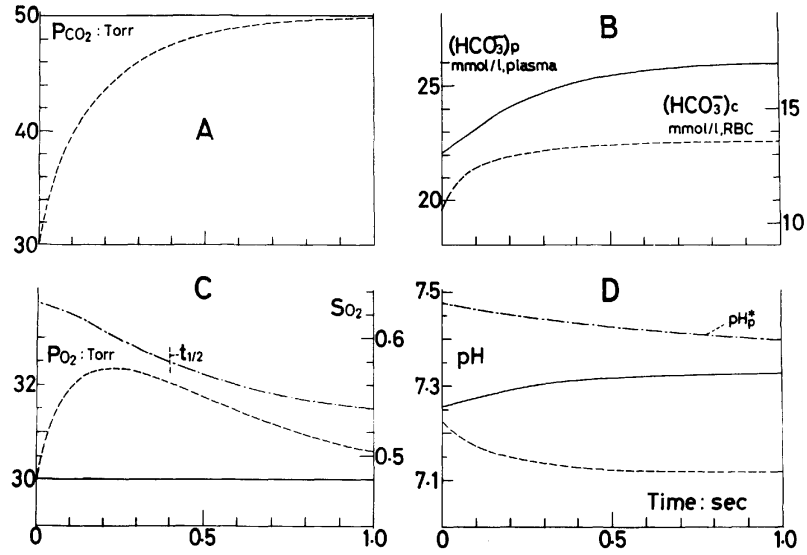

Fig. 5. Overall gas exchange profiles during the Bohr-off-shift in an open vessel. The solid and broken lines represent the respective values in the extra- and intracellular fluid. The chain line in graph C is the S_{O_2}. The extracellular P_{O_2} was maintained at 30 Torr.

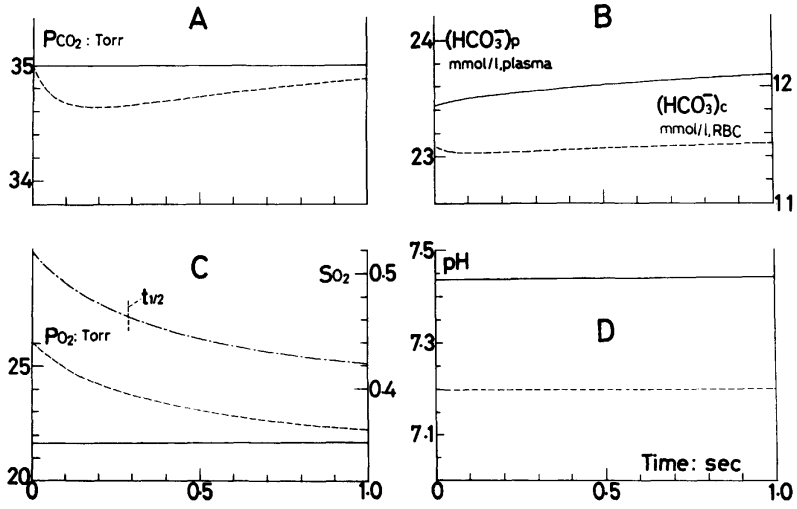

Fig. 6. Overall gas exchanges profiles during the deoxygenation in an open system. The extracellular P_{O_2} was reduced from 26 to 21.7 Torr, thus, making the changing S_{O_2} range equal to that of the Bohr-off-shift in Fig. 5. The extracellular P_{CO_2} was maintained at a level of 45 Torr.

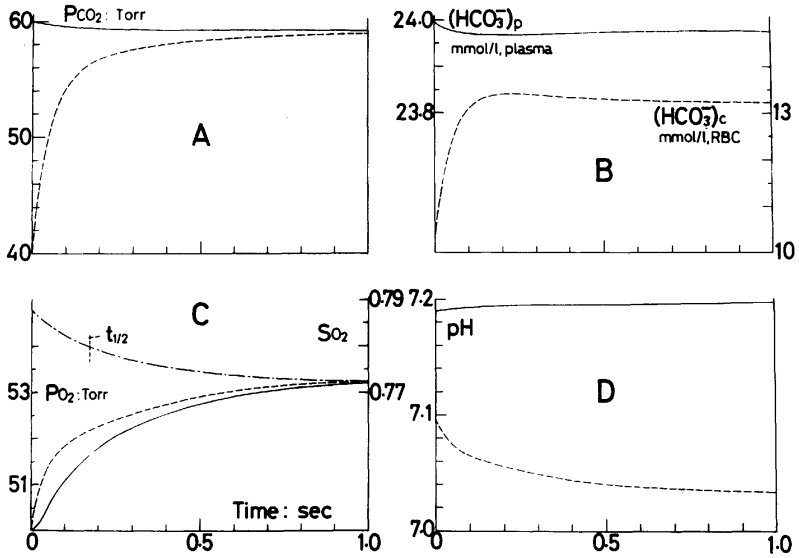

Fig. 7. Overall gas exchange profiles during the Bohr-off-shift in a closed system. Both the intra- and extracellular P_{O_2} increased, while the S_{O_2} decreased from the initial value of 0.78. The hematocrit was 0.015, and the extracellular P_{CO_2} was changed from 40 to 60 Torr.

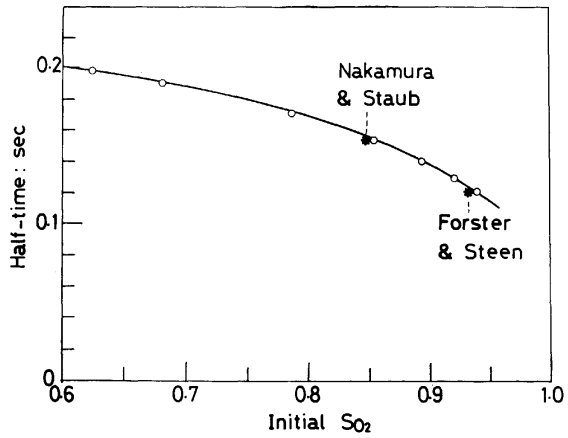

Fig. 8. Relationship between the half-time and initial S_{O_2} obtained in the computation of the Bohr-off-shift in a closed system, where the hematocrit is 0.015, and the extracellular P_{CO_2} was changed from 40 to 60 Torr.

tracellular HCO_3^- content was calculated from Eqs. (2) and (5) by using the initial intracellular P_{CO_2} and P_{O_2}, whereas the initial extracellular HCO_3^- was invariably taken to be 24 mmol·l(plasma)$^{-1}$. An example of the overall gas exchange profiles is shown in Fig. 7, where the initial P_{O_2} is 50 Torr. Following the rise in intracellular

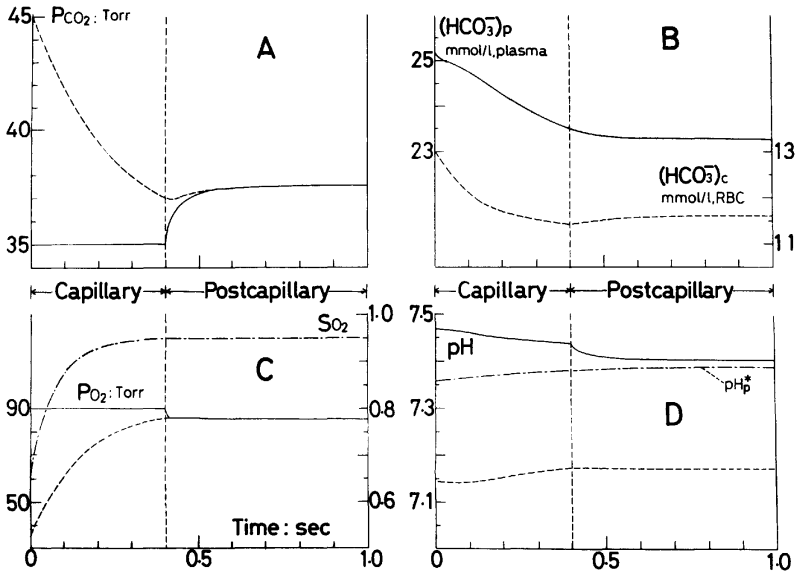

Fig. 9. Overall gas exchange profiles during the oxygenation accompanying the outward CO_2 diffusion in normal blood with a hematocrit of 0.45. The extracellular P_{O_2} was changed from 35 to 90 Torr, while the extracellular P_{CO_2} was reduced from 45 to 35 Torr. The chain line in graph D represents the change in pH_p* which corresponds to that of the buffer-base of plasma protein.

P_{CO_2}, the extracellular P_{O_2} increased. According to the outward O_2 diffusion, the S_{O_2} decreased from 0.787 to 0.773. The half-time of the S_{O_2} change was almost the same as that of the extracellular P_{O_2}, being less than one half of the value in the open system (Fig. 5). Figure 8 shows the relation of half-time to the initial S_{O_2}. The half-time value decreased as the S_{O_2} value increased. NAKAMURA and STAUB (1964) and FORSTER and STEEN (1968) measured the Bohr-off-shift to have an initial S_{O_2} value of 0.85 and 0.93, respectively. They obtained an average half-time value of 0.152 and 0.12 s, respectively, which was compatible with the computed data shown by the solid line. The half-time value measured by CRAW *et al.* (1963) at a Ht of 0.09 and at an initial S_{O_2} of 0.95 was 0.14 s, which was a little longer than the computed value. This difference may be attributed to the difference in the Ht value.

3) Gas exchange profiles computed in a pulmonary capillary model

Using the same parameter values as shown in Tables 1 and 2, we calculated the changes in P_{O_2}* and S_{O_2}, P_{CO_2}, HCO_3^- content, and pH in the pulmonary capillary model. In order to simplify the computation, the capillary wall was assumed to be fully permeable with the O_2 and CO_2 diffusions. The following boundary and initial conditions were adopted: Alveolar $P_{O_2}=90$ Torr, mixed venous $P_{O_2}=35$ Torr, alveolar $P_{CO_2}=35$ Torr and mixed venous $P_{CO_2}=45$ Torr. Presuming that an exercise state exists, the contact time was taken to be 0.4 s. After passing through the

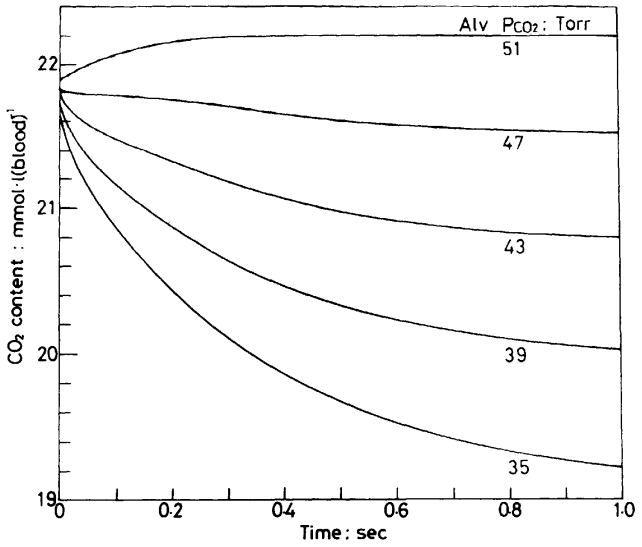

Fig. 10. CO_2 content in blood computed during the transit time in the pulmonary capillary model. The mixed venous P_{CO_2} was invariably 45 Torr, and the alveolar P_{CO_2} ranged from 35 to 51 Torr, sequentially. The extracellular P_{O_2} was changed from 35 to 90 Torr.

capillary, the RBC was assumed to have entered the closed system, where the time constant of extracellular carbonic anhydrase activity was taken to be 1.5 s.

Figure 9 shows the overall gas exchange profiles in the pulmonary capillary, where oxygenation and outward CO_2 diffusion take place simultaneously. As described before, A, B, C, and D show the changes in P_{CO_2}, HCO_3^- content, P_{O_2}* and S_{O_2}, and pH, respectivley. The rate of the P_{O_2}* change, 105 ms in half-time, was much slower than that of S_{O_2}. This paradoxical phenomenon may partly be deduced from the S_{O_2} dependency of the rate factor of hemoglobin oxygenation, F_s(ox), as shown in Table 1. The half-time of the intracellular $P_{CO_2}$was 170 ms, and that of the intracellular HCO_3^- was 110 ms, obviously shorter than that of the extracellular HCO_3^-, which was 280 ms.

The above data show that the CO_2 output is slower than that of oxygenation in the pulmonary capillary. To illustrate the relationship between the venous and arterial CO_2 content difference and the contact time, we further calculated the total CO_2 change in blood along with the transit time. The mixed venous P_{CO_2} and P_{O_2} values were invariably 45 and 35 Torr, respectively. The alveolar P_{CO_2} changed within the range of 35 to 51 Torr, whereas the alveolar P_{O_2} remained constant at 90 Torr. The computed profiles of CO_2 content are shown in Fig. 10. Except at an alveolar P_{CO_2} range higher than 47 Torr, the CO_2 content in blood does not seem to reach the equilibrium state within 1 s. When the alveolar P_{CO_2} equalled 47 Torr, despite the initial inversed P_{CO_2} gradient across the RBC boundary outward CO_2, diffusion occurred due to the Haldane effect. Namely, oxygenation occurred faster

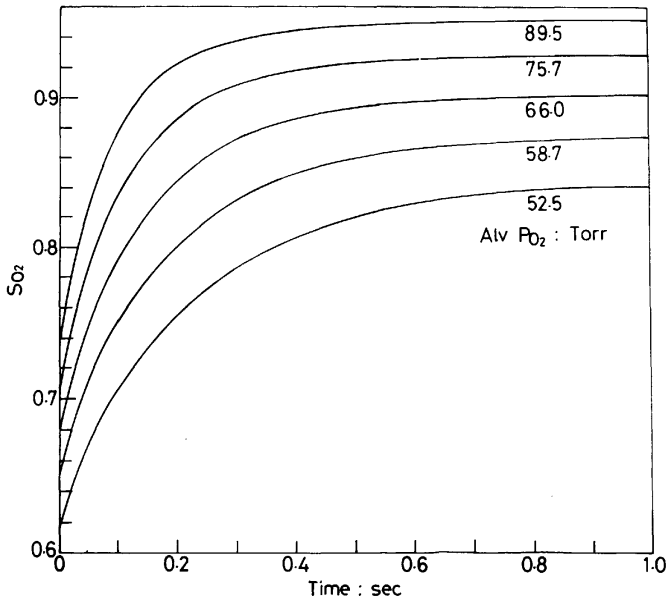

Fig. 11. S_{O_2} profiles during the transit time using the pulmonary capillary model. Both the venous and alveolar P_{O_2} were varied so as to keep the arterial venous O_2 content difference at 4.6 vol%. The P_{CO_2} ranged from 40 to 45 Torr. The $\eta(O_2)$ was reduced to 1.5×10^{-6} cm·s^{-1}·Torr^{-1}, whereas $\eta(CO_2) = 2.5 \times 10^{-6}$ cm·s^{-1}·Torr^{-1}.

than outward CO_2 diffusion. When hypercapnia of the alveolar P_{CO_2} equalled 51 Torr, the half-time value was shorter than 100 ms.

The oxygenation rate of RBC, however, occurs fairly quickly, compared with the CO_2 output. Figure 11 shows the S_{O_2} profiles computed by varying both the mixed venous and alveolar P_{O_2}, so that the venous-arterial O_2 content difference was kept at 4.6 vol%. The mixed venous and alveolar P_{CO_2} were invariably taken to be 45 and 40 Torr, respectively. The $\eta(O_2)$ was assumed to be 1.5×10^{-6} s^{-1}·Torr^{-1}, referring to the relation in extracellular diffusion constant between O_2 and CO_2 and the transfer coefficient for CO ($= 1.2 \times 10^{-6}$ s^{-1}·Torr^{-1}) estimated in normal subjects by MOCHIZUKI *et al.* (1972) and KAGAWA and MOCHIZUKI (1982). Despite the low $\eta(O_2)$ value, the oxygenation is almost completed within the contact time of 0.4 s in normoxia. Even with a hypoxia of 52.5 Torr in alveolar P_{O_2}, 85% of the oxygenation is accomplished within the contact time of 0.4 s. In contrast, the venous-arterial CO_2 content difference at the contact time of 0.4 s is about 80% that of the 1 s contact.

DISCUSSION

In the case of the O_2 and CO diffusions in the RBC, linearized partial

differential equations were solved analytically by MOCHIZUKI (1975) using a two dimensional disc model. Since then, we have computed the changes in S_{O_2}, S_{CO}, and extracellular pH, using the disc model, and determined the permeabilities of O_2, CO, CO_2, and HCO_3^- across the RBC boundary by comparing the numerical solution with the experimental data. Subsequently, the simultaneous differential equations for O_2, CO_2, and HCO_3^- diffusions were solved in the same model. In addition, the diffusion coefficients of CO_2 and HCO_3^- were also estimated experimentally by ourselves. We also derived the formulas of the Haldane- and Bohr-effects from the measured dissociation curves. Hence, it may be safe to say that the numerical solutions in the present study are all based on the measured data, and almost free from the difference in shape between the RBC and the model.

One of the major problems in deriving the overall gas exchange rates in the RBC was to evaluate the buffer value of hemoglobin, β_c. When the β_c value is estimated from the CO_2 dissociation curves of whole blood and true plasma, a small variation in CO_2 content causes a great error in the β_c value. Previously, we approximated the CO_2 dissociation curve with a single exponential function (MOCHIZUKI *et al.*, 1982). Such an approximation, however, was not accurate enough to derive the β_c value. The CO_2 content at a P_{CO_2} range lower than 15 Torr usually deviated from the exponential curve. Therefore, we determined β_c solely from the CO_2 contents in a P_{CO_2} range of 20 to 100 Torr. The β_c value used was $62\,\text{mmol}\cdot l(\text{RBC})^{-1}\cdot \text{pH}^{-1}$ at a pH_c of 7.17 or a pH_p of 7.4, which was compatible with the previous data (SIGGAARD-ANDERSEN, 1971; TAKIWAKI *et al.*, 1983; SHIMOUCHI *et al.*, 1984).

In the present computation, the time constant of CO_2-dehydration (or hydration) reaction due to capillary carbonic anhydrase was taken to be 1.5 s. When the time constant of 1 s is used in the calculation of Fig. 10, the calculated change in CO_2 content in the blood becomes about $0.02\,\text{mmol}\cdot l(\text{blood})^{-1}$ greater at 1 s of contact time than the value illustrated in the same figure. Therefore, the error in time constant may be permissible. As shown in Figs. 4 to 8, the computed extracellular P_{O_2} and P_{CO_2} curves due to the Haldane- and Bohr-effects are in strong agreement with the experimental data. This coincidence seems to support the applicability of the present numerical solution in the O_2 and CO_2 diffusions, at least in the normal lung.

REFERENCES

BARTELS, H., BETKE, K., HILPERT, P., NIEMEYER, G., and RIEGEL, K. (1961) Die sogenannte Standard-O_2-Dissoziationskurve des gesunden erwachsenen Menschen. *Pflügers Arch.*, **272**: 372–383.

BAUER, C. (1974) On the respiratory function of hemoglobin. *Rev. Physiol. Biochem. Pharmacol.*, **70**: 1–31.

BAUER, C., and SCHRÖDER, E. (1972) Carbamino compounds of hemoglobin in human adult and fetal blood. *J. Physiol. (Lond.)*, **227**: 457–471.

CRAW, M. R., CONSTANTINE, H. P., MORELLO, J. M., and FORSTER, R. E. (1963) Rate of the

Bohr shift in human red cell suspensions. *J. Appl. Physiol.*, **18**: 317–324.

DOUGLAS, J., Jr. and RACHFORD, H. H., Jr. (1956) On the numerical solution of the heat conduction problems in two and three space variables. *Trans. Am. Math. Soc.*, **82**: 421–439.

FORSTER, R. E. and STEEN, J. B. (1968) Rate limiting processes in the Bohr shift in human red cells. *J. Physiol. (Lond.)*, **296**: 541–562.

KAGAWA, T. (1984) Programs for Solving O_2 and CO_2 Diffusions into and out of the Erythrocyte, ed. by MOCHIZUKI, M., Yamagata Med. Soc., Yamagata, pp. 1–149.

KAGAWA, T. and MOCHIZUKI, M. (1982) Numerical solution of partial differential equation describing oxygenation rate of the red blood cell. *Jpn. J. Physiol.*, **32**: 197–218.

KAGAWA, T. and MOCHIZUKI, M. (1984) Numerical solution of partial differential equations for CO_2 diffusion accompanying HCO_3^- shift in red blood cells. *Jpn. J. Physiol.*, **34**: 1029–1047.

KLOCKE, R. A. (1973) Mechanism and kinetics of the Haldane effect in human erythrocyte. *J. Appl. Physiol.*, **35**: 673–681.

KLOCKE, R. A. (1978) Catalysis of CO_2 reactions by lung carbonic anhydrase. *J. Appl. Physiol.*, **44**: 882–888.

MOCHIZUKI, M. (1966a) Study on the oxygenation velocity of the human red cell. *Jpn. J. Physiol.*, **16**: 635–648.

MOCHIZUKI, M. (1966b) On the velocity of oxygen dissociation of human hemoglobin and red cell. *Jpn. J. Physiol.*, **16**: 649–657.

MOCHIZUKI, M. (1975) Graphical Analysis of Oxygenation and CO-Combination Rates of the Red Cells in the Lung, Hirokawa Publ. Co., Tokyo., pp. 1–71.

MOCHIZUKI, M., FUKUI, K., and NAKABAYASHI, T. (1972) Diffusibility of CO across the diffusion layer around the red cell flowing through the pulmonary capillary. *In*: Advances in Respiratory Physiology and Controls, *Monogr. Ser. Res. Inst. Appl. Electr., Hokkaido Univ.*, **20**, 79–89.

MOCHIZUKI, M. and FUKUOKA, J. (1958) The diffusion of oxygen inside the red cell. *Jpn. J. Physiol.*, **8**: 206–224.

MOCHIZUKI, M., NAKAMURA, K., and OYAMA, Y. (1966) Study on the oxygenation velocity of human hemoglobin. *Jpn. J. Physiol.*, **18**: 519–527.

MOCHIZUKI, M., TAKIWAKI, H., KAGAWA, T., and NIIZEKI, K. (1983a) Estimation of the rate of CO_2 diffusion into the red cell through the Bohr shift. *In*: Oxygen Transport to Tissue. IV, ed. by BICHER, H. I. and BRULEY, D. F., Plenum Press, New York, pp. 509–518.

MOCHIZUKI, M., TAKIWAKI, H., KAGAWA, T., and TAZAWA, H. (1983b) Derivation of theoretical equations of the CO_2 dissociation curve and the carbamate fraction in the Haldane effect. *Jpn. J. Physiol.*, **33**: 579–599.

MOCHIZUKI, M., TAZAWA, H., and TAMURA, M. (1982) Mathematical formulation of CO_2 dissociation curve and buffer line of human blood at rest. *Jpn. J. Physiol.*, **32**: 231–244.

NAKAMURA, T. and STAUB, N. (1964) Synergism in the kinetic reactions of O_2 and CO_2 with human red blood cells. *J. Physiol. (Lond.)*, **173**: 161–177.

NIIZEKI, K., MOCHIZUKI, M., and KAGAWA, T. (1984) Secondary CO_2 diffusion following the HCO_3^- shift across the red blood cell membrane. *Jpn. J. Physiol.*, **34**: 1003–1013.

NIIZEKI, K., MOCHIZUKI, M., and UCHIDA, K. (1983) Rate of CO_2 diffusion in the human red blood cell measured with pH-sensitive fluorescence. *Jpn. J. Physiol.*, **33**: 635–650.

SHIMOUCHI, A., MOCHIZUKI, M., and NIIZEKI, K. (1984) Change in P_{CO_2} in red cell suspension following bicarbonate shift. *Jpn. J. Physiol.*, **34**: 1015–1027.

SIGGAARD-ANDERSEN, O. (1971) Oxygen-linked hydrogen ion binding of human hemoglobin. Effects of carbon dioxide and 2,3-diphosphoglycerate. I. Studies on erythrolysate, and II. Studies on whole blood. *Scand. J. Clin. Lab. Invest.*, **27**: 351–360, 361–366.

TAKIWAKI, H., MOCHIZUKI, M., and NIIZEKI, K. (1983) Relationship between hematocrit and CO_2 contents in whole blood and true plasma. *Jpn. J. Physiol.*, **33**: 567–578.

TAZAWA, H., MOCHIZUKI, M., TAMURA, M., and KAGAWA, T. (1983) Quantitative analyses of the CO_2 dissociation curve of oxygenated blood and the Haldane effect in human blood. *Jpn. J. Physiol.*, **33**: 601–618.

UCHIDA, K., MOCHIZUKI, M., and NIIZEKI, K. (1983) Diffusion coefficients of CO_2 molecule and bicarbonate ion in hemoglobin solution measured by fluorescence technique. *Jpn. J. Physiol.*, **33**: 619–634.

VAN SLYKE, D. D., WU, H., and MCLEAN, F. C. (1923) Studies of gas and electrolyte equilibria in the blood. V. Factors controlling the electrolyte and water distribution in the blood. *J. Biol. Chem.*, **106**: 765–839.

VAN SLYKE, D. D., HASTINGS, A. B., HILLER, A., and SENDROY, J., Jr. (1928) Studies of gas and electrolyte equilibria in blood. XIV. The amounts of alkali bound by serum albumin and globulin. *J. Biol. Chem.*, **79**: 769–780.